Quantum transduction via frequency upconversion (Invited)

Aaron P. VanDevender and Paul G. Kwiat

Department of Physics, University of Illinois at Urbana-Champaign, 1110 W Green Street, Urbana, Illinois 61801, USA

Received September 22, 2006; revised October 13, 2006; accepted October 15, 2006; posted October 19, 2006 (Doc. ID 75334); published January 26, 2007

We describe a method for efficiently and coherently converting photons from one wavelength to another through the process of nonlinear upconversion. By using an intense 1064 nm escort laser pulse and a periodically poled lithium niobate (PPLN) crystal, we demonstrate upconversion efficiency of 99% and coherence of 95% for 1550 to 631 nm light at the single-photon level, thereby qualifying it for use in manipulation of photonic qubits. We then show how to create photons in arbitrary superpositions of different energy states, thereby enlarging the accessible Hilbert space for quantum information applications. © 2007 Optical Society of America

OCIS codes: 190.7220, 270.1670.

1. INTRODUCTION

Since the prediction by Armstrong *et al.*[1] that multiple optical wavelengths could be mixed using nonlinear dielectric media, upconversion[2] has been successfully used in a wide variety of classical optical applications, including narrowband infrared (IR) imaging,[3] blackbody thermal imaging,[4] IR[5] and time-resolved[6] spectroscopy, as well as detection of IR sources from the near IR (e.g., 1550 nm) to the very deep IR[7] (e.g., 10.6 μm). These techniques may also be employed in improved single-molecule detection[8] and low-light IR astronomy.[9]

Now frequency upconversion promises to enhance and enable several quantum information technologies where the promise of optical qubits is greatly enriched by the ability to shift their wavelengths to desired values.[10–15] For example, high-efficiency single-photon detectors that utilize frequency upconversion of telecommunication-wavelength photons could substantially increase the range and data rates of quantum cryptography systems that rely on the faithful transmission and receipt of IR single-photon quantum states.[16] Upconversion may also be used to prepare complex quantum states by partially upconverting a photon into an arbitrary superposition of two frequencies. This, in addition to polarization, angular momentum, and time bin, provides another degree of freedom for transmitting quantum information. Finally, future quantum networks will likely require the ability to freely change between the wavelength of a particular "flying" qubit (e.g., a telecommunication-wavelength photon) and a "stationary" qubit (e.g., a trapped atom or quantum dot). This type of quantum "transduction" may have an important role in distributed quantum computation[17] and quantum communication.[18]

For upconversion to be suitable for use in these applications, however, two properties must be demonstrated. First, the process must be efficient at the single-photon level—we must have the capability to convert nearly all of one frequency to another frequency reliably and with low loss. Here we demonstrate a high-efficiency frequency upconversion process from 1550 to 631 nm.[14] We also use this technique to produce photons in arbitrary superpositions of these two widely separated frequencies, thereby displaying high-contrast "Rabi oscillations" between the two energy states.

The second requirement is that the process be coherent—if phase information is lost during the transduction process, the state of the qubit being transferred will not be preserved. Previous experiments have demonstrated that the photon statistics of the beam are preserved in the upconversion process.[19] Here we demonstrate the coherence of the process by preparing a weak 1550 nm pulse in a superposition of two time-bin states, upconverting to the visible, and measuring the high-visibility interference fringes between the two time-bin states of the upconverted photon.[20]

2. UPCONVERSION BACKGROUND

Other work on high-efficiency upconversion has employed continuous pumping beams, using either a buildup cavity[11] or nonlinear crystals with waveguide structures[10,20] to achieve the high intensities required. Our scheme instead relies on using bright escort *pulses* in a bulk, quasi-phased-matched periodically poled lithium niobate (PPLN) crystal, thus avoiding the insertion loss of waveguide structures and cavities and leading to reduced background.

The nonlinear field evolution for this process was given by Myers *et al.*,[21] from which we calculate the quantum-state evolution and the probability of upconversion $P_o(z)$:

$$P_o(z) = \sin^2\left(\sqrt{\frac{\omega_i \omega_o d_Q^2 |E_e|^2}{n_i n_o c^2}} z \right), \tag{1}$$

where ω_i and ω_o are the input and output angular frequencies; n_i and n_o are the indices of refraction of the in-

 © 2007 Optical Society of America

put and output beams, respectively; d_Q is the effective nonlinear coefficient; and E_e is the amplitude of the escort electric field. By choosing an appropriate crystal length L such that $P_o(L)=1$, one can in principle achieve near-unity conversion efficiency. The efficiency in practice is limited by losses and how well one can match the spatial, spectral, and temporal modes of the interfering light fields.

3. HIGH-EFFICIENCY CONVERSION

As shown in Fig. 1, our 1550 nm photons are combined on a dichroic beam splitter with very bright escort pulses from a passively Q-switched Nd:YAG laser that produces 600 ps wide pulses at 1064 nm. A variable attenuator allows us to modulate the intensity of the escort pulse, which is then focused to a spot at the midpoint of a PPLN crystal. The 1550 nm light (from a telecom diode laser) is passed through a pair of waveguide electro-optic intensity modulators (EOM), creating pulses that are 200 ps wide. The EOM is triggered by the escort laser, thereby synchronizing the 1550 nm pulse to the escort. A calibrated attenuator reduces the mean number of photons per pulse to <1, thus closely approximating a superposition of a single-photon Fock state and the vacuum (under the assumption that our laser outputs a coherent state; however, see, e.g., Pegg and Jeffers[22] and references therein). Since the probability of upconversion $P_o(z)$ depends on the intensity of the escort ($|E_e|^2$), and our pulsed escort necessarily has a time-varying intensity, we make the input pulse much shorter than the escort pulse so that the input photon experiences only the (relatively constant) peak intensity of the escort. However, the 1550 nm pulse duration cannot be too short, or the concomitant spread in frequencies will fall outside the phase-matching bandwidth for efficient upconversion. The input beam is then focused inside the crystal onto the center of the escort beam spot.

After the PPLN, the upconverted photon (now at 631 nm) passes through a series of low-loss Brewster-cut dispersion prisms and a high-transmission interference filter (centered at 631 nm) to remove the remaining 1064 nm light and some 532 nm background (created from parasitic second-harmonic generation of the escort laser). Finally, the upconverted light is detected using a silicon avalanche photodiode (APD). By knowing the initial rate of IR photons, and the collection and detection efficiencies of our system, we can determine the conversion efficiency. With this system, operating at ~40 kHz, we have seen conversion efficiencies of up to 99±4%.

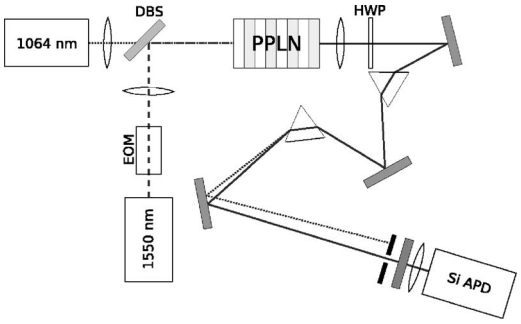

Fig. 1. High-efficiency upconversion experiment. A weak 1550 nm pulse is combined on a dichroic beam splitter (DBS) with a bright 1064 nm escort pulse and focused onto a nonlinear crystal (PPLN). The 631 nm upconverted pulse is then filtered through dispersion prisms and an interference filter and finally detected by a silicon avalanche photodiode (APD). HWP, half-wave plate.

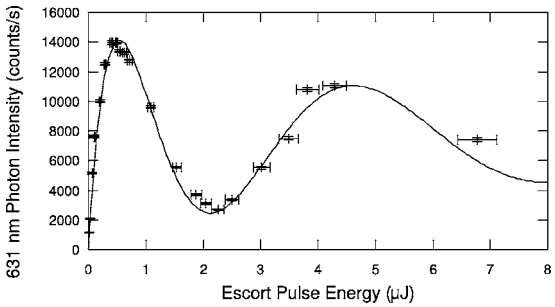

Fig. 2. Rabi oscillation-like nature of upconversion [Eq. (1)] is demonstrated by measuring the rate of upconverted photons for increasing escort pulse intensities. The imperfect visibility is well modeled (solid curve) by the precise pulse shapes. Visibility is limited mostly by the extent to which the 1544 nm pulse is temporally and spatially smaller than the escort pulse. The prediction was scaled in the pulse-energy direction owing to inability to measure the absolute peak escort intensity to better than a factor of 2; however, predicted and measured pulse energies agree to that level.

4. RABI OSCILLATIONS

For a fixed crystal length, we can rewrite Eq. (1) as $\sin^2(KE_e)$, equivalent to a Rabi oscillation (mediated by the escort field strength) between the input and the output energy states. Figure 2 shows the number of detected upconverted photons for various escort intensities, along with a (single free parameter) theoretical prediction obtained by integrating the field-evolution equations given by Myers *et al.*[21] and including the effect of the measured pulse shapes of the escort and input photons. The measured temporal profile of the input pulse includes a long non-Gaussian tail owing to the device limitations of the EOM used to create it. This leads to a reduced visibility in Fig. 2, since not all of the input light falls within the peak intensity of the escort pulse. For this experiment we used $\lambda=1544$ nm pulses focused to a ~100 μm spot in a 4.5 cm crystal. A 220 μm wide 1064 nm beam was chosen to maximize the number of Rabi fringes at the expense of some visibility. The maximum predicted conversion efficiency at the first Rabi peak is 98%. However, extreme filtering was required to suppress background for escort pulse energies more than an order of magnitude above what is necessary for maximum conversion (e.g., 7 μJ). The detector and filtering efficiencies were each at about 65%, and the average number of photons per pulse was 0.95. This gives an overall system-detection efficiency of about 41%, which is comparable to other efforts.[15] By instead optimizing focusing for conversion efficiency (e.g., a 350 μm escort beam gives a predicted conversion efficiency above 99%), using the minimum escort energy required for maximum conversion efficiency, and reducing the level of spectral filtering (so that collection efficiency =87%), we have observed a total system-detection effi-

ciency of 56%, which we believe is the highest reported, with a background level of $\sim 10^{-2}$ dark counts per detection window.

It is also possible to overconvert the photons so that they transition $1544 \rightarrow 630 \rightarrow 1544$ nm (a previous experiment demonstrated some upconversion dependence on escort intensity but was unable to document the predicted oscillations[12]). Our data clearly show that we can control the conversion probability by varying the escort intensity. In this way, we can prepare quantum states that are arbitrary superpositions of the two frequency states: $\alpha|630\text{ nm}\rangle \exp(-i\omega_{630}t) + \beta|1544\text{ nm}\rangle \exp(-i\omega_{1544}t)$. We know of no other method to efficiently produce such nondegenerate photon states, which may have use in quantum networking protocols, e.g., protocols requiring coupling to stationary nondegenerate qubits, or in protocols where time-dependent qubits may be desirable. By invoking the polarization dependence of the upconversion process, one can create even more complicated quantum states residing in a larger Hilbert space.

5. COHERENCE

To investigate the coherence of the upconversion process, we send both a 1550 nm photon and the escort pulse through an unbalanced interferometer (see Fig. 3). The path-length difference of the long and short arms (1.4 m) is much greater than the pulse width of both the escort and 1550 nm pulses. In this way we prepare a coherent superposition of two time bins for the 1550 nm photon. After upconversion of the photon amplitude in each time bin, we use a second interferometer to verify that the upconversion process has preserved the phase coherence between the time bins. The exiting upconverted photon can be detected at one of three possible times. The earliest (latest) arrival times correspond to distinguishable events where the photon traveled the short (long) arms on both trips through the interferometer. The short–long and long–short processes contributing to the middle time bin will interfere if, and only if, the upconversion process preserves the coherence of the time-bin qubit.

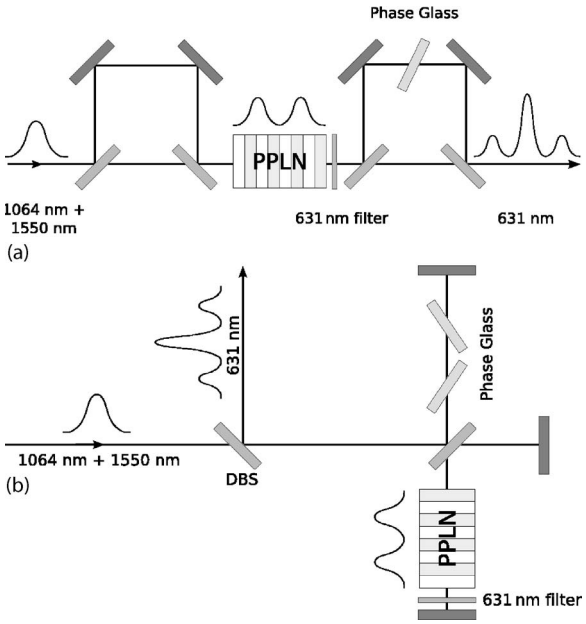

Fig. 3. (a) Preparation of 1550-nm pulse along with a bright 1064 nm escort pulse in a two-time-bin superposition state using an unbalanced Mach–Zehnder interferometer. The photon is upconverted and then passed through another interferometer with a phase shifter in one arm. Interference fringes are observed in the resulting middle time bin. (b) An equivalent, but more robust, implementation using an unbalanced Michelson interferometer. After the two-time-bin state is prepared and upconverted, it is reflected back through the interferometer and picked off using a dichroic beam splitter, where it is detected by an APD. Two dispersive glass plates are tipped near Brewster's angle to produce a low-loss and zero walk-off phase shift between the long–short and short–long processes.

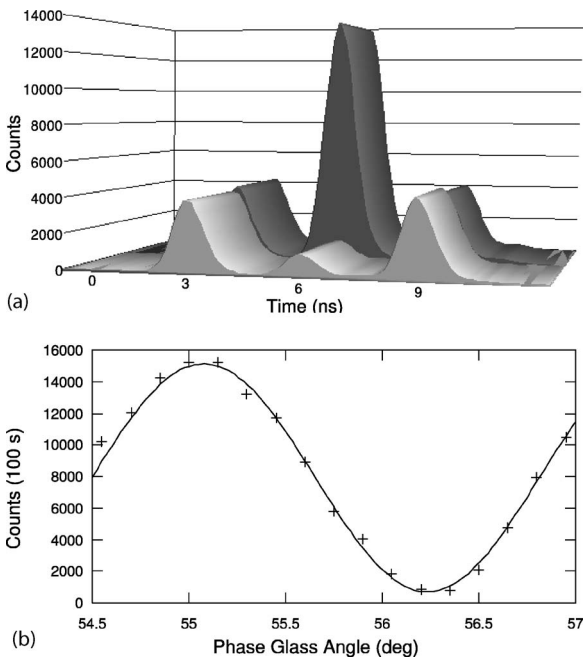

Fig. 4. (a) Detected photons versus time for two settings of the phase glass, corresponding to constructive and destructive interference. The long–long and short–short processes are unaffected by the position of the phase glass, while the central time bin, arising from the interfering short–long and long–short processes, varies greatly. (b) Number of photons detected in the central time bin as the phase glass plates are tilted. The visibility fringe is 95% and demonstrates the coherence of the upconversion process.

For our experiment we used a double-pass Michelson interferometer [Fig. 3(b)]. We initially focus both beams onto a "virtual waist" 15 cm before the interferometer beam splitter. The (spherical) end mirrors on each arm image this virtual waist onto the center of a 1.5 cm crystal, allowing both beams in both arms to be focused onto the same point (for this experiment they all had approximately the same spot size, $\sim 60\ \mu$m). The upconverted output at 631 nm is directed through an identical unbalanced interferometer; for stability we simply reflect the photon back through the *same* crystal and interferometer (a filter removes the other wavelengths) so that any path-length fluctuations affect both the short–long and long–short processes identically. Upon re-exiting the interferometer, the 631 nm light is separated out from the remaining escort light using a dichroic beam splitter, dispersion prisms, and interference filters.

The phase is controlled by tipping two 1 mm thick glass plates in the long arm. The glass is dispersive, and in

each process different wavelengths pass through the glass, causing a relative phase shift between the short–long and the long–short processes. Figure 4(a) shows the time histogram of the detected photons for two extremal values of the phase shift. Figure 4(b) shows the number of photons detected versus the angle of the phase glass, along with a theoretical fit using only the initial phase and visibility as free parameters. The fit visibility is $95 \pm 1\%$, without subtracting background counts, indicating that the transduction process indeed preserves the coherence of the time-bin qubit. Similar time-bin-conserving upconversion has also recently been demonstrated using PPLN waveguides[20]; however, waveguide coupling losses limited the net conversion efficiency to less than 10%.

This two-time-bin encoding is precisely that used by most fiber-based quantum cryptography efforts,[18,23–26] which, moreover, also rely on attenuated pulses to approximate single-photon states. Our present level of interference contrast would correspond to an approximate key distribution bit error rate of 2.5%, comparable to that reported with existing systems. Note also that in principle these upconversion methods can allow superior detection time resolution, limited only by the escort pulse duration and not by the detector response jitter.

6. CONCLUSION

Now that we have the capability to convert efficiently and coherently between different frequency states, we can consider coupling the frequency basis with other degrees of freedom (e.g., time bin, polarization, etc.) to produce complex quantum states.[27] For example, by coupling a frequency qubit with a time-bin qubit, we can create states of the form $\alpha|f_1,S\rangle + \beta|f_1,L\rangle + \gamma|f_2,S\rangle + \delta|f_2,L\rangle$, where S and L represent the two time-bin states. Such states, which occupy a much larger Hilbert space than single time-bin states (six-dimensional for a pure state with two time-bins and two frequencies), could be very useful for advanced quantum communication protocols, e.g., where larger quantum alphabets enhance security.[28]

The conversion efficiency and coherence visibility reported here for weak coherent states should apply equally well to true single-photon states. The entanglement preservation results obtained by Tanzilli *et al.*[20] should also apply to our system, thus allowing it to be used in applications requiring entangled single photons. Furthermore, by upconverting in bulk, we avoid the insertion losses associated with waveguides, yielding a higher net conversion efficiency.

Obviously, the technique demonstrated here can be easily extended to other input and output frequencies by selecting the appropriate escort frequency and poling period. There is also the potential to combine this scheme with microwave-pump upconversion (which has demonstrated $\sim$100 GHz shifts[29]) and electro- and acousto-optic modulation techniques. This would provide fine-tuning control (e.g., for coupling to an atomic system) on top of the coarse frequency control achieved here.

ACKNOWLEDGMENT

This work was supported by the MURI Center for Photonic Quantum Information Systems (ARO/DTO program DAAD19-03-1-0199).

Corresponding author A. P. VanDevènder can be reached by e-mail at vandvndr@uiuc.edu.

REFERENCES

1. J. A. Armstrong, N. Bloembergen, J. Ducuing, and P. S. Pershan, "Interactions between light waves in a nonlinear dielectric," Phys. Rev. **127**, 1918–1939 (1962).
2. G. D. Boyd and D. A. Kleinman, "Parametric interaction of focused Gaussian light beams," J. Appl. Phys. **39**, 3597–3639 (1968).
3. J. E. Midwinter, "Image conversion from 1.6 μm to the visible in lithium niobate," Appl. Phys. Lett. **12**, 68–70 (1968).
4. K. F. Hulme and J. Warner, "Theory of thermal imaging using infrared to visible image up-conversion," Appl. Opt. **11**, 2956–2964 (1972).
5. T. R. Gurski, H. W. Epps, and S. P. Maran, "Upconversion of broadband infrared spectra," Appl. Opt. **17**, 1238–1242 (1978).
6. R. Schanz, S. A. Kovalenko, V. Kharlanov, and N. P. Ernsting, "Broad-band fluorescence upconversion for femtosecond spectroscopy," Appl. Phys. Lett. **79**, 566–568 (2001).
7. J. Warner, "Spatial resolution measurements in up-conversion from 10.6 μm to the visible," Appl. Phys. Lett. **13**, 360–362 (1968).
8. F. V. Bright, "Modern molecular fluorescence spectroscopy," Appl. Spectrosc. **49**, 14A–19A (1995).
9. M. M. Abbas, T. Kostiuk, and K. W. Ogilvie, "Infrared upconversion for astronomical applications," Appl. Opt. **15**, 961–970 (1976).
10. R. V. Roussev, C. Langrock, J. R. Kurz, and M. M. Fejer, "Periodically poled lithium niobate waveguide sum-frequency generator for efficient single-photon detection at communication wavelengths," Opt. Lett. **29**, 1518–1520 (2004).
11. M. A. Albota and F. N. C. Wong, "Efficient single-photon counting at 1.55 μm by means of frequency upconversion," Opt. Lett. **29**, 1449–1451 (2004).
12. G. Giorgi, P. Mataloni, and F. De Martini, "Frequency hopping in quantum interferometry: efficient up–down conversion for qubits and ebits," Phys. Rev. Lett. **90**, 027902 (2003).
13. K. Karstad, A. Stefanov, M. Wegmuller, H. Zbinden, N. Gisin, T. Aellen, M. Beck, and J. Faist, "Detection of mid-IR radiation by sum frequency generation for free space optical communication," Opt. Lasers Eng. **43**, 537–544 (2005).
14. A. P. VanDevender and P. G. Kwiat, "High efficiency single photon detection via frequency up-conversion," J. Mod. Opt. **51**, 1433–1445 (2004).
15. C. Langrock, E. Diamanti, R. V. Roussev, Y. Yamamoto, and M. M. Fejer, "Highly efficient single-photon detection at communication wavelengths by use of upconversion in reverse-proton-exchanged periodically poled $LiNbO_3$ waveguides," Opt. Lett. **30**, 1725–1727 (2005).
16. K. Inoue, E. Waks, and Y. Yamamoto, "Differential phase shift quantum key distribution," Phys. Rev. Lett. **89**, 037902 (2002).
17. M. A. Nielsen and I. L. Chuang, *Quantum Computation and Quantum Information* (Cambridge U. Press, 2000).
18. N. Gisin, G. Ribordy, W. Tittel, and H. Zbinden, "Quantum cryptography," Rev. Mod. Phys. **74**, 145–195 (2002).
19. J. Huang and P. Kumar, "Observation of quantum frequency conversion," Phys. Rev. Lett. **68**, 2153–2156 (1992).
20. S. Tanzilli, W. Tittel, M. Halder, O. Alibart, P. Baldi, N. Gisin, and H. Zbinden, "A photonic quantum information interface," Nature **437**, 116–120 (2005).
21. L. E. Myers, R. C. Eckardt, M. M. Fejer, R. L. Byer, W. R. Bosenberg, and J. W. Pierce, "Quasi-phase-matched optical parametric oscillators in bulk periodically poled $LiNbO_3$," J. Opt. Soc. Am. B **12**, 2102–2116 (1995).

22. D. T. Pegg and J. Jeffers, "Quantum nature of laser light," J. Mod. Opt. **52**, 1835–1856 (2005).
23. R. J. Hughes, G. L. Morgan, and C. G. Peterson, "Quantum key distribution over a 48-km optical fiber network," J. Mod. Opt. **47**, 533–547 (2000).
24. D. Stucki, N. G. O. Guinnard, G. Ribordy, and H. Zbinden, "Quantum key distribution over 67 km with a plug&play system," New J. Phys. **4**, 41.1–41.8 (2002).
25. See MagiQ Technologies at http://www.magiqtech.com/.
26. See id Quantique at http://www.idquantique.com/.
27. J. T. Barreiro, N. K. Langford, N. A. Peters, and P. G. Kwiat, "Generation of hyperentangled photon pairs," Phys. Rev. Lett. **95**, 260501 (2005).
28. C. Wang, F. G. Deng, Y. S. Li, X. S. Liu, and G. L. Long, "Quantum secure direct communication with high-dimension quantum superdense coding," Phys. Rev. A **71**, 044305 (2005).
29. D. A. Farías and J. N. Eckstein, "Dynamic electrooptic frequency shifter for pulsed light signals," IEEE J. Quantum Electron. **41**, 94–99 (2005).